Applied Surface Science 479 (2019): 260-264

DOI: https://doi.org/10.1016/j.apsusc.2019.02.020

DFT Molecular Dynamics and Free Energy Analysis of a Charge Density Wave Surface System

Daniel G. Trabada, Jesús I. Mendieta-Moreno,
Diego Soler-Polo, Fernando Flores, and José Ortega
Departamento de Física Teórica de la Materia Condensada and Condensed Matter Physics Center (IFIMAC), Facultad de Ciencias, Universidad Autónoma de Madrid, E-28049 Madrid, Spain

(Dated: January 30, 2019)

Abstract

The K/Si(111):B $\sqrt{3} \times \sqrt{3}$ surface, with one K atom per $\sqrt{3} \times \sqrt{3}$ unit cell, is considered a prototypical case of a surface Mott phase at room temperature. Our Density Functional Theory (DFT) Molecular Dynamics (MD) and free energy calculations show, however, a $2\sqrt{3} \times \sqrt{3}$ Charge Density Wave (CDW) ground state. Our analysis shows that at room temperature the K atoms easily diffuse along the lines of a honeycomb network on the surface and that the $\sqrt{3} \times \sqrt{3}$ phase appears as the result of the dynamical fluctuations between degenerate CDW states. DFT-MD free energy calculations also show a $2\sqrt{3} \times \sqrt{3} \leftrightarrow \sqrt{3} \times \sqrt{3}$ transition temperature below 90K. The competing electron-electron and electron-phonon interactions at low temperature are also analyzed; using DFT calculations, we find that the electron-phonon negative-U^* is larger than the electron-electron Hubbard U, indicating that the CDW survives at very low temperature.

1. INTRODUCTION

Metal layers on semiconductors present many different reconstructions [1] and new structures [2, 3], as well as competing exotic phenomena [4–7] including Mott phases [8–10] and Charge Density Waves (CDW) [11–13]. Although static Density Functional Theory (DFT) calculations provide a good starting point for the study of these systems, atomic dynamics usually play an important role and DFT Molecular Dynamics (MD) simulations are required to further understand the behaviour of the system [14]. For a more complete description of the system, however, entropy and free energy should be considered [15, 16]. Still, free energy calculations require the statistical sampling of a large number of DFT configurations [17]; this is a challenging problem, explaining why for surface systems only a few DFT free energy 1D profiles have been determined [18, 19]. Moreover, at very low temperatures electron-electron and/or electron-phonon many-body effects can be important, effects that are not accurately described in standard DFT techniques.

In this work we analyze the atomic dynamics and many-body properties for a surface case study, K/Si(111):B $\sqrt{3} \times \sqrt{3}$ with one K atom per $\sqrt{3} \times \sqrt{3}$ unit cell ($\theta = 1/3$ ML), that shows a $\sqrt{3} \times \sqrt{3}$ geometry and is nonmetallic at room temperature [20]; this was interpreted as an indication of the appearance of a Mott phase on the surface. However, the analysis of the Si $2p$ and B $1s$ core levels as a function of coverage [21] indicates that, for $\theta = 1/3$, the surface has two types of B atoms, and Si adatoms, with equal weight. For a slightly larger K coverage, $\theta = 1/2$ ML, a $2\sqrt{3} \times 2\sqrt{3}$ phase is observed [6, 21–23]; this structure presents 3 Si adatoms displaced upwards and one Si adatom displaced downwards [6]. Our DFT calculations reveal that a similar CDW distortion appears for $\theta = 1/3$ ML. In order to reconcile these results with the experimental observation of a $\sqrt{3} \times \sqrt{3}$ ($\sqrt{3}$ in the following) phase at room temperature, we perform very long DFT-MD simulations at different temperatures. These simulations show that at room temperature the system jumps between degenerate $2\sqrt{3} \times \sqrt{3}$ CDW states; as a result of these dynamical fluctuations [14, 24–26], the $\sqrt{3}$ phase can be understood as the dynamical average of the different CDW structures the system visits, in agreement with the core-level data [21]. These DFT-MD simulations also show that the K atoms present a very important diffusive motion along the surface that promotes the up/down fluctuations of the Si adatoms. Thus, we calculate the free energy 2D map for the transition between two different CDW states using the Weighted

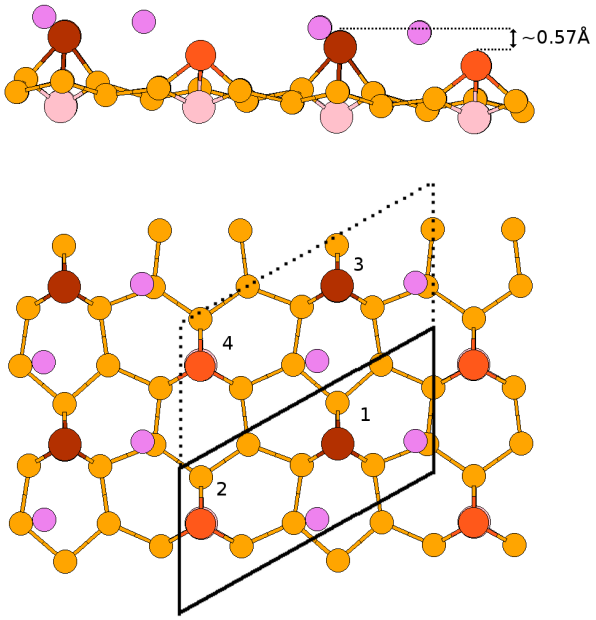

FIG. 1. Color online. Top and side view for the K/Si(111):B $2\sqrt{3} \times \sqrt{3}$ atomic structure. Large brown and orange circles represent up and down Si adatoms; the vertical distortion is $\Delta z = 0.57$ Å. B atoms (pink circles) are located below the Si adatoms. The K atoms (purple circles) easily diffuse on this surface. Only the two upper Si layers are shown, for clarity. The solid and dashed black lines indicate the $2\sqrt{3} \times \sqrt{3}$ and $2\sqrt{3} \times 2\sqrt{3}$ unit cells.

Histogram Analysis Method (WHAM) [27, 28]. From all these calculations we estimate a $2\sqrt{3} \times \sqrt{3} \leftrightarrow \sqrt{3}$ transition temperature lower than 90K. In order to analyze the low T limit, we perform constrained DFT calculations to determine the electron-electron, U, and electron-phonon, λ, interactions, that with the mean frequency, w_0, of the Si adatoms, as obtained in our DFT-MD simulations, define the parameters of an effective Hubbard-Holstein hamiltonian [29, 30]. We find that the negative U^*, defined as $2\lambda^2/w_0$, is around 15 % larger than the repulsive U, suggesting that the CDW found at high and moderate T survives at very low T [31, 32].

2. DFT METHODS

In our theoretical approach we combine accurate plane-waves DFT calculations and computationally efficient local-orbital DFT-MD simulations. In particular, we use the plane-

waves QUANTUM ESPRESSO (QE) simulation package [33] for the determination of the surface geometries and energy differences. Using this code, however, for the DFT-MD simulations and free energy calculations presented in this work is prohibited by its computational and time-consuming cost. Therefore, these DFT-MD simulations are performed with the FIREBALL code [34–36] using Numerical Atomic-like Orbitals (NAOs) [37] optimized to reproduce the QE results.

In the QE DFT calculations the one-electron wave-functions were expanded in a basis set of plane-waves, with energy cut-off of 80 Ry, using the BLYP exchange-correlation functional [38, 39] and Goedecker-Teter-Hutter pseudopotentials [40]; the K $3p$ semi-core states were included explicitly in the calculation. A vacuum region in the z-direction of ~ 40 Å was employed. The Brillouin zone (BZ) (in the XY plane) was sampled by means of Monkhorst-Pack (MP) grids; in particular, for the $2\sqrt{3} \times 2\sqrt{3}$ surface a (4×4) MP grid yields fully converged results. The DFT-MD simulations are performed with the local-orbital FIREBALL code using a $2\sqrt{3} \times 2\sqrt{3}$ unit cell (see Fig. 1) and a 2×2 MP special k-point grid, which practically yields converged results for relaxed geometries and energy differences. We use an optimized sp^3-basis set of Numerical Atomic-like Orbitals [37] for Si and B, while for K we have included a p^3s basis representing the $3p$ semi-core and the $4s$ valence orbitals. The Si orbitals were optimized for the description of bulk Si; the B orbitals were fitted to reproduce the CDW $2\sqrt{3}\times\sqrt{3}$ and $\sqrt{3}\times\sqrt{3}$ atomic structures, as well as the energy difference between them, as obtained in the accurate QE calculations, see below.

The K/Si(111):B surface was modelled by a slab with 6 full Si (111) layers plus the Si adatom layer on T4 positions; the B atoms are located on the second Si layer, replacing the Si atoms placed below the Si adatoms. The lower Si layer was saturated by H atoms; the lower two Si layers and the H atoms are fixed in the calculations. In total, there are 92 atoms in the $2\sqrt{3} \times 2\sqrt{3}$ unit-cell. All calculations have been performed using the corresponding theoretical lattice constant, $a = 5.46$ Å (QE) and $a = 5.50$ Å (FIREBALL).

3. RESULTS AND DISCUSSION

3.1 Charge Density Wave

Figure 1 shows the K/Si(111):B $2\sqrt{3}\times\sqrt{3}$ atomic structure as calculated with QE. In the Si(111):B-$\sqrt{3}$ surface the Si adatom dangling bonds are empty due to the B delta doping. When K atoms are added to this surface they transfer their valence electron to the Si dangling bonds; in the ideal $\sqrt{3}$ geometry all the Si adatoms are equivalent and their dangling bonds are filled with one electron; thus, a half occupied surface band appears at the Fermi energy [41](Figure 2a). Our calculations show that this ideal geometry is unstable w.r.t. a $2\sqrt{3}\times\sqrt{3}$ CDW with Si adatoms displaced up/down, with a vertical distortion $\Delta z = 0.57$ Å. The B-Si adatom bond length also shows a large vertical relaxation [6], d(B-Si$_{up}$) = 2.95 Å and d(B-Si$_{down}$) = 2.19 Å. This CDW state is lower in energy than the $\sqrt{3}$ case by 0.35 eV per $2\sqrt{3}\times\sqrt{3}$ unit cell. The CDW distortion is accompanied by a displacement of the K atoms towards the up Si adatoms (Si$_{up}$), promoting the transfer of one electron between Si$_{down}$ and Si$_{up}$ dangling bonds. Accordingly, the half occupied surface band is split into two bands, one fully occupied and the other empty, separated by 0.8 eV (Figure 2b).

The CDW state is sixfold degenerate, depending on which particular pair of Si adatoms are up or down. Thus, in the next step we have performed DFT-MD simulations at different temperatures to explore the possible dynamical fluctuations between CDW states. For this purpose we use the local-orbital FIREBALL code, less accurate than QE but much more computationally efficient. As mentioned above, in these DFT-MD simulations the basis set is fitted to reproduce the QE results; we obtain $\Delta z = 0.5$ Å, d(B-Si$_{up}$) = 2.92 Å, d(B-Si$_{down}$) = 2.22 Å, and an energy difference between the $\sqrt{3}$ and CDW structures of 0.35 eV, to be compared with the QE values presented above (also, see Supplementary Material).

3.2 DFT-MD simulations

We have performed DFT-MD simulations at different temperatures: T= 150K, 300K, 400K, 450K and 600K, for a $2\sqrt{3}\times 2\sqrt{3}$ unit cell with 4 Si adatoms (see Figure 1). The time step is $\Delta t = 1.5$ fs and the total simulation time ranges between 200 ps and 1000 ps in the different simulations, see Table I. Figure 3 illustrates the up/down time evolution of the Si adatoms, represented by means of the following generalized coordinates: α =

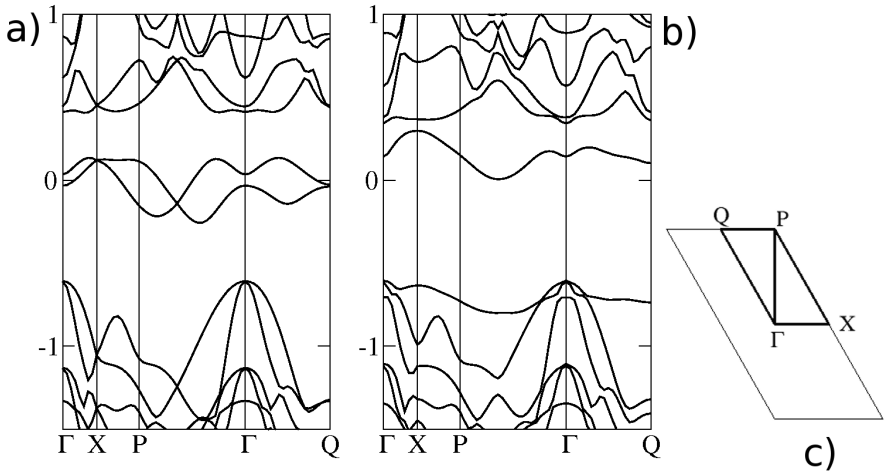

FIG. 2. Electronic energy bands (in eV) for the (a) K/Si(111):B-$\sqrt{3}$ and (b) $2\sqrt{3} \times \sqrt{3}$ surfaces, both represented using a $2\sqrt{3} \times \sqrt{3}$ unit-cell for an easier comparison. A narrow half occupied surface band is found in the $\sqrt{3}$-case (a); this band appears as two bands at the Fermi level (0 eV) due to the doubling of the unit cell. In the CDW structure (b) this band is split into two narrow bands separated by ~ 0.8 eV. (c) reciprocal space unit-cell and directions.

$\frac{1}{2}(z_1 + z_2 - z_3 - z_4)$; $\beta = \frac{1}{2}(z_1 - z_2 + z_3 - z_4)$; $\gamma = \frac{1}{2}(z_1 - z_2 - z_3 + z_4)$, defined in terms of the vertical (z) displacements of the 4 Si adatoms; the mean displacement of the adatoms, $(z_1 + z_2 + z_3 + z_4)/4$ is not represented since it presents no interesting feature. At T = 300K (Fig. 3a) the system is oscillating around the initial state, $\alpha \approx 0.5$ Å, $\beta \approx \gamma \approx 0$, which is one of the six possible CDW states (Si adatoms 1 and 2 up, and adatoms 3 and 4 down). The behaviour for T = 150K (not shown) is similar, with no fluctuations between different CDW states all along the simulation time, ~ 1000 ps. At T = 400K (Fig. 3b), the system shows several fluctuations between different CDW states; for instance, after around 220 ps the system jumps from the initial state to a different CDW configuration, $\gamma \approx -0.5$ Å, $\alpha \approx \beta \approx 0$ (adatoms 2 and 3 up, and adatoms 1 and 4 down); in total there are 7 jumps in ~ 710 ps; these jumps appear in a chaotic fashion and are extremely fast. At higher temperatures (T = 450K and 600K) these fluctuations take place more frequently, see Figs. 3(c,d) and Table I. These results suggest that at high temperature the Si adatoms present ultrafast fluctuations, in which two of them jump simultaneously, one moving down

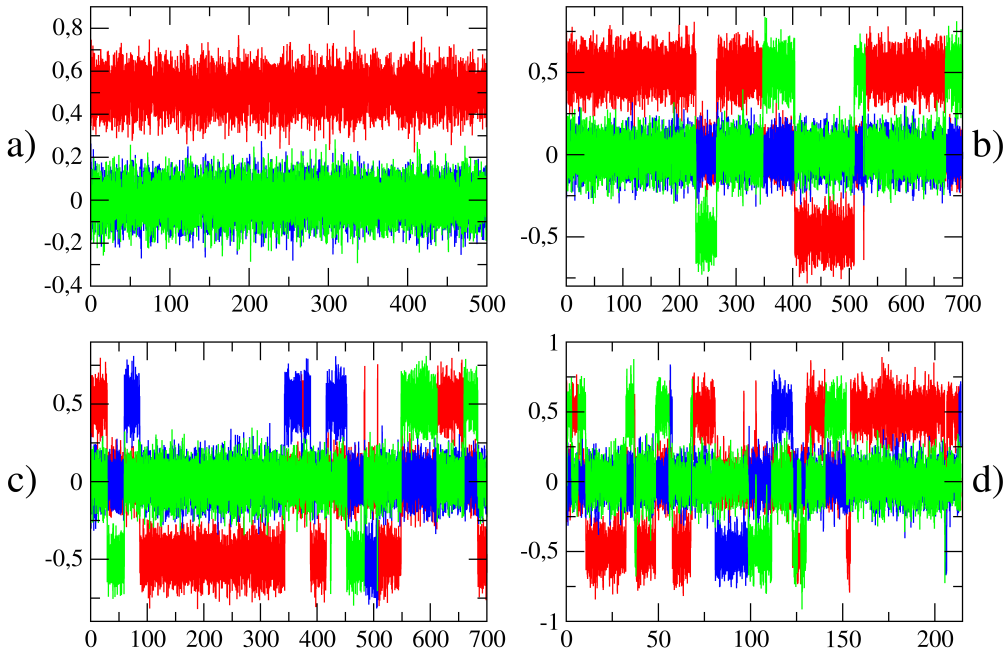

FIG. 3. Color online. Up/down motion of the Si adatoms in the DFT-MD simulations: $\alpha(t)$ (red), $\beta(t)$ (blue) and $\gamma(t)$ (green), (in Å) for (a) T = 300K, (b) T = 400K, (c) T = 450K and (d) T = 600K (time in ps). At T = 400K, 450K and 600K the system jumps between the six degenerate CDW configurations in a chaotic way. Notice the different time scales (x-axis) for the different cases.

and the other moving up, the system visiting in this way all the degenerate CDW states. These fluctuations appear in a random way, because one *e.g.* Si_{up} can be coupled in this motion with anyone of the neighbouring Si_{down}. These dynamical fluctuations explain why the system presents, on average, a $\sqrt{3}$-symmetry [20] and at the same time two different types of Si adatoms and B atoms are observed [21].

3.3 Free energy map

In these DFT-MD simulations we find that the K atoms easily diffuse on the Si(111):B surface [42], following the lines of a honeycomb pattern around the Si adatoms (see Sup-

T (K)	N_f	t_s (10^{-12} s)	τ (s)	$\tau^* = t_s/N_f$ (s)
600	27	210	6.9×10^{-12}	7.8×10^{-12}
450	17	720	4.5×10^{-11}	4.2×10^{-11}
400	7	710	1.1×10^{-10}	1.0×10^{-10}
300	-	500	1.9×10^{-9}	$> 5.0 \times 10^{-10}$
150	-	1030	1.5×10^{-4}	$> 1.0 \times 10^{-9}$
$T_c = 94 - 83$			$\tau_c = 10^2 - 10^4$	

TABLE I. Estimation of the transition temperature T_c using an Arrhenius-like equation $\tau = C \exp(\Delta G/k_B T)$ for the mean fluctuation time. The value of $\Delta G = 0.29$ eV is obtained from Figure 4, and the constant C from the results shown in Figure 3 for T = 400K, 450K and 600K ($C = 2.5 \times 10^{-14}$ s). N_f is the number of fluctuations and t_s the total simulation time for each temperature T.

plementary Material). This finding indicates the convenience of calculating the *free energy* of the system instead of the total energy to properly take into account the effects of the diffusion of the K atoms (as well as the vibrations of all the surface atoms) on the phase transition. Therefore, we have calculated a DFT free energy map at T = 450K using the Umbrella Sampling technique [27]. The reaction coordinates are the z-coordinates of two of the Si-adatoms in the unit cell (*e.g.* atoms 1 and 2 in Fig. 1) while the z-coordinates of the other two Si adatoms are restrained by means of additional umbrella potentials, in such a way that one remains in an up position and the other in a down position. In this way we generate a huge number of configurations ($\sim 1.3 \times 10^6$) using DFT-MD and calculate the free energy map by means of the WHAM method [28]. In particular, we have used a 36 $\times$ 36 grid of umbrella windows and $\sim$ 1000 configurations per window; the constant used for the umbrella potentials is $k = 600$ kcal/mol Å^{-2}. Figure 4 shows this free energy map; the free energy barrier between the two minima is 0.29 eV, 0.06 eV lower than the static barrier (total energy difference between the CDW and $\sqrt{3}$ configurations). The minimum energy path corresponds to the anti-symmetric displacement $z_2 = -z_1$. The transition state corresponds to a local $\sqrt{3}$-geometry for the two Si adatoms, with $z_1 = z_2 = 0$.

It is interesting to use the DFT-MD and free energy results (Figures 3 and 4) to estimate the transition temperature, T_c, between the fluctuating $\sqrt{3}$-phase and the CDW structure.

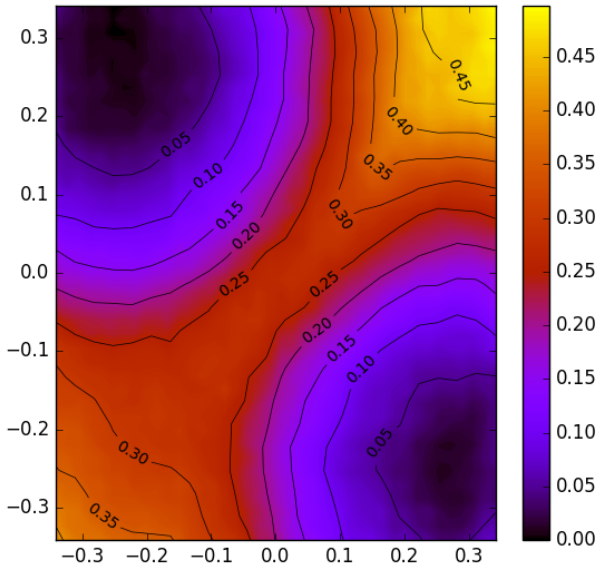

FIG. 4. Color online. Free energy map, in the $(2\sqrt{3} \times 2\sqrt{3})$-unit cell, as a function of the (z_1, z_2) reaction coordinates (in Å). The two minima at (z_1, z_2) = (-0.25, 0.25) Å and (0.25, -0.25) Å correspond to two different CDW ground states. The free energy barrier is around 0.29 eV.

For this purpose we use an Arrhenius-like equation for the mean fluctuating time, $\tau = C \exp(\Delta G/k_B T)$, with $\Delta G = 0.29$ eV and C a constant determined from the results of Figure 3, and assume that this transition is defined by taking $\tau \sim 10^2 - 10^4$ s. This procedure is justified by the exponential nature of the equation; as shown in Table I, this yields $T_c \approx 90\text{K} \pm 7\text{K}$.

3.4 Mapping to a Hubbard-Holstein model

So far we have discussed the nature of the observed $\sqrt{3}$ phase at RT. At very low T other exotic phases might appear, different from the CDW obtained in the DFT calculations. The large vertical CDW distortions, Δz and d(Si-B), and large splitting of the surface bands (Figure 2) suggest, however, that the CDW is the stable phase even at very low T. We have further analyzed this low T limit by mapping our DFT calculations into a Hubbard-Holstein hamiltonian [29, 30]:

$$\hat{H}_{HH} = \sum_{(i,j),\sigma} t\hat{c}^{+}_{i\sigma}\hat{c}_{j\sigma} + \sum_{i} U\hat{n}_{i\uparrow}\hat{n}_{i\downarrow} + \sum_{i} w_0(\hat{b}^{+}_{i}\hat{b}_i + 1/2) + \sum_{i} \lambda\hat{n}_i(\hat{b}^{+}_{i} + \hat{b}_i), \qquad (1)$$

where U is the Hubbard electron-electron interaction, λ represents the electron-phonon interaction associated with a local phonon defined by its frequency w_0, and t is the nearest neighbor hopping interaction. This hamiltonian has been used to analyze systems with important electron-phonon and electron-electron interactions.

DFT calculations can be used to obtain the parameters appearing in this hamiltonian. The nearest-neighbor hopping t is obtained from a fitting to the DFT $\sqrt{3}\times\sqrt{3}$ surface bands (Fig. 2a), $t \approx 40$ meV, while the frequency w_0 can be obtained from the vertical vibrations of the Si adatoms in the DFT-MD simulations (*e.g.* see Fig. 3 and Supplementary Material); for this purpose we have taken an average of the frequencies found in the simulations for different temperatures and obtain $w_0 \approx 21 \pm 1.5$ meV. In order to obtain U and λ we perform constrained DFT calculations, fixing the Kohn-Sham orbital occupations [43], whereby the surface bands of the CDW structure keep the same charge as in the $\sqrt{3}$ surface (*i.e.* all dangling bonds are half-occupied). We obtain a gap between the upper and lower surface bands of $E_g \approx 1.2$ eV. This yields $U^* = 2\lambda^2/w_0 \approx 1.1$ eV, where we have used $\lambda = \frac{\Delta E}{\Delta x}(\hbar/(2Mw_0))^{1/2}$, with ΔE the shift of the surface bands as a function of the adatom displacements Δx, and $M \approx \frac{4}{3}M_{Si}$ [44]. U^* is the effective negative-U contribution due to the electron-phonon interaction [29, 30].

Finally, the Hubbard U is obtained from a comparison of the band splitting E_g mentioned above with the band splitting, $E_g' \approx 0.8$ eV, shown in Figure 2b (that corresponds to fully occupied and empty surface bands). This yields $U = (U^0 - J) \approx 0.95$ eV. In this equation J is the nearest neighbor electron-electron interaction, which is obtained with the help of an electrostatic model [43] in which the Si surface is described as a semi-infinite medium with a dielectric constant of 11.9, and U^0 is the on-site electron-electron interaction ($U^0 \approx 1.28$ eV). These values can be compared with $U^0 = 1.1$ eV, $J = 0.5$ eV and $U = 0.6$ eV as obtained in ref. [45]. These results show that $U/t \approx 24$, $U^*/t \approx 28$, $U^* > U$, and $w_0/t \approx 0.5$, values that also suggest that the CDW is the stable solution at T = 0K [29, 30, 46]. In particular, we find that the electron-phonon effective negative-U is larger than the Hubbard U, $U^* > U$, by ~ 15 %. This discussion shows that either a Mott-phase or an antiferromagnetic structure can be excluded as appearing for K/Si(111):B at low T.

As a further test we calculate the correlation energy associated with the half-filled band of Fig. 2a, not included appropriately in the DFT calculations. This energy can be written as [12, 47] $E_{corr} = -\frac{1}{4}fU$, $0 < f < 1$, where f depends on U/W, W being the bandwidth

of the two dimensional electron gas (see Fig. 2a), with $f = 1$ for a highly correlated system ($U/W >> 1$) and $f = 0$ in the opposite limit ($U/W << 1$). In our system $W = 0.36$ eV, and we find from other similar cases [12, 47] that $f \approx 0.39$ and $E_{corr} = -0.09$ eV per adatom, for $U = 0.95$ eV (or $f \approx 0.28$ and $E_{corr} = -0.04$ eV for $U = 0.6$ eV [45]). This correlation energy should be compared with the energy of the CDW geometry with respect to the $\sqrt{3}$-surface, -0.35 eV (per two adatoms), still indicating that the CDW is the stable phase. That correlation energy reduces, however, the energy barrier for the dynamical fluctuations (Fig. 4) and also T_c below 90K.

4. CONCLUSIONS

In conclusion, we have analyzed the K/Si(111):B ($\theta = 1/3$) surface by means of long DFT-MD simulations and free energy calculations involving a huge number of configurations. Our results show that a CDW is the ground state of the system. The $\sqrt{3}$ phase observed at room temperature is due to the dynamical fluctuations of the system between different CDW states; these fluctuations are coupled to the motion of the K atoms, that easily diffuse following a honeycomb pattern along the surface. Entropy and electron correlations reduce the free energy barrier for the up/down fluctuations of the Si adatoms. We also show that the negative-U^* is larger than U, indicating that the CDW survives at very low T.

Acknowledgements

This work was supported by Grants No. MAT2014-59966-R and MAT2017-88258-R from the Spanish MINECO.

[1] P.C. Snijders and H.H. Weitering, Rev. Mod. Phys. **82**, 307 (2010).

[2] J.Y.Lee, J.H. Cho and Z. Zhang, Phys. Rev. B **80**, 155329 (2009).

[3] S. Okada, K. Shiraishi and A. Oshiyama, Phys. Rev. Lett. **90**, 026803 (2003).

[4] T. Zhang *et al.*, Nat. Phys. **6**, 104 (2010).

[5] A. Tejeda, Y. Fagot-Revurat, R. Cortés, D. Malterre, E.G. Michel and A. Mascaraque, Phys. Status Solidi A **209**, 614 (2012).

[6] L. Chaput *et al.*, Phys. Rev. Lett. **107**, 187603 (2011).

[7] J.Z. Zhao *et al.*, Phys. Rev. Lett. **117**, 116101 (2016).

[8] M. Rolhfing and J. Pollmann, Phys. Rev. Lett. **84**, 135 (2000).

[9] R. Cortés *et al.*, Phys. Rev. Lett. **96**, 126103 (2006).

[10] Fangfei Ming *et al.*, Phys. Rev. Lett. **119**, 266802 (2017).

[11] J.M. Carpinelli, H.H. Weitering, M. Bartkowiak, R. Stumpf and E.W. Plummer, Phys. Rev. Lett. **79**, 2859 (1997).

[12] R. Cortés *et al.*, Phys. Rev. B **88**, 125113 (2013).

[13] HW Yeom *et al.*, Phys. Rev. Lett. **82** 4898 (1999).

[14] J. Ávila *et al.*, Phys. Rev. Lett. **82** 442 (1999).

[15] C. Chipot, A. Pohorille (Eds.), *Free Energy Calculations*, (Springer, Berlin 2007).

[16] S. Wippermann and W.G. Schmidt, Phys. Rev. Lett. **105**, 126102 (2010).

[17] N. Hansen and W.F. van Gunsteren, J. Chem. Theory Comput. **10**, 2632 (2014).

[18] P. Minary and M.E. Tuckerman, J. Am. Chem. Soc. **126**, 13920 (2004).

[19] V.M. Sánchez, J.A. Cojulun and D.A. Scherlis, J. Phys. Chem. C **114**, 11522 (2010).

[20] H.H. Weitering *et al.*, Phys. Rev. Lett. **78**, 1331 (1997).

[21] Y. Fagot-Revurat *et al.*, J. Phys. Condens. Matter **25**, 094004 (2013).

[22] L.A. Cardenas, Y. Fagot-Revurat, L. Moreau, B. Kerrien and D. Malterre, Phys. Rev. Lett. **103**, 046804 (2009).

[23] Y. Fukaya, I. Mochizuki and A. Kawasuso, Phys. Rev. B **86**, 035423 (2012).

[24] C. González, F. Flores and J. Ortega, Phys. Rev. Lett. **96**, 136101 (2006).

[25] D.G. Trabada and J. Ortega, J. Phys. Condens. Matter **21**, 182003 (2009).

[26] W. Srour *et al.*, Phys. Rev. Lett. **114**, 196101 (2015).

[27] G.M. Torrie and J.P. Valleau, J. Comput. Phys. **23**, 187 (1977).

[28] S. Kumar *et al.* J. Comput. Chem. **13**, 1011 (1992).

[29] W. Koller, D. Meyer and A.C. Hewson, Phys. Rev. B **70**, 155103 (2004).

[30] A. Macridin, G.A. Sawatzky and M. Jarrell, Phys. Rev. B **69**, 245111 (2004).

[31] G. Allan and M. Lannoo, Phys. Rev. Lett. **66**, 1209 (1991).

[32] O. Pankratov and M. Scheffler, Phys. Rev. Lett. **71**, 2797 (1993).

[33] P. Giannozzi *et al.* J. Phys.:Condens. Matter **21**, 395502 (2009).

[34] J.P. Lewis, P. Jelínek, J. Ortega, A.A. Demkov, D.G. Trabada, B. Haycock, Hao Wang, G. Adams, J.K. Tomfohr, E. Abad, Hong Wang and D.A. Drabold, Phys. Status Solidi B **248**,

1989 (2011).

[35] J.P. Lewis, K.R. Glaesemann, G.A. Voth, J. Fritsch, A.A. Demkov, J. Ortega, O. F. Sankey, Phys Rev B **64**, 195103 (2001).

[36] P. Jelínek, H. Wang, J.P. Lewis, O.F. Sankey, J. Ortega, Phys Rev B **71**, 235101 (2005).

[37] M.A. Basanta, Y.J. Dappe, P. Jelínek and J. Ortega, Comput. Mater. Sci. **39**, 759 (2007).

[38] A.D Becke, Phys. Rev. A **38**, 3098 (1988).

[39] C. Lee, W. Yang, and R. G. Parr Phys. Rev. B **37**, 785 (1988).

[40] S. Goedecker, M. Teter and J. Hutter, Phys. Rev. B **54**, 1703 (1996).

[41] H.Q. Shi, M.W. Radny and P.V. Smith, Phys. Rev. B **70**, 235325 (2004).

[42] Kyeongjae Cho and E. Kaxiras, Surface Science **396**, L261 (1998).

[43] J. Ortega, F. Flores and A. Levy Yeyati, Phys. Rev. B **58**, 4584 (1998).

[44] R. Pérez, J. Ortega and F. Flores, Phys. Rev. Lett. **86**, 4891 (2001).

[45] P. Hansmann, T. Ayral, L. Vaugier, P. Werner and S. Biermann, Phys. Rev. Lett. **110**, 166401 (2013).

[46] S. Karakuzu, L.F. Tocchio, S. Sorella and F. Becca, Phys Rev B **96**, 205145 (2017).

[47] P. Pou *et al.*, Phys. Rev. B **62**, 4320 (2000).